*This is the Author Accepted Manuscript (postprint) of the following paper:*

# Deformation Twinning in $Au_{30}Ag_{70}$ Alloy Nanowires under Tensile Strain

Wonsik Kim[a], Kkotchorong Park[b], Seung Jo Yoo[a,c], Paolo Matteini[d], Byungil Hwang[e*],

Bongsoo Kim[b*], and Seung Min Han[a*]

[a] Department of Material Science and Engineering, Korea Advanced Institute of Science and Technology, Daejeon 34141, Republic of Korea

[b] Department of Chemistry, Korea Advanced Institute of Science and Technology, Daejeon 34141, Republic of Korea

[c] Electron Microscopy Research Center, Korea Basic Science Institute (KBSI), Daejeon 34133, Republic of Korea

[d] Institute of Applied Physics "Nello Carrara", National Research Council, Via Madonna del Piano 10, Sesto Fiorentino 50019,Italy

[e] School of Integrative Engineering, Chung-Ang University, Seoul, 06974, Republic of Korea

*Corresponding authors: bihwang@cau.ac.kr, bongsoo@kaist.ac.kr, smhan01@kaist.ac.kr

KEYWORDS. Twinning, AuAg, Alloy, Nanowire, Tensile

ABSTRACT

Defect-free AuAg alloy nanowires have the potential to be used in various plasmonic devices due to their superior chemical stability and broad applicable range of wavelengths. Alloyed nanowires have different stacking fault energies that can result in different deformation behavior compared to single element nanowires; however, an in-depth analysis of such material system is yet to be explored. In this study, defect-free single crystalline $Au_{30}Ag_{70}$ alloy nanowires are synthesized by topotaxial growth method and tested in tension using an *in-situ* pico-indenter. Deformation twinning that results in superplastic deformation of alloy nanowires is experimentally observed. The critical dimension of $Au_{30}Ag_{70}$ alloy nanowires at which transition from ordinary plasticity to deformation twinning occurs?, is experimentally determined to be ~333 nm, which is about 2 time larger than that of Au nanowires. Stacking fault energy, which is the key element determining the deformation mode, of $Au_{30}Ag_{70}$ alloy nanowires is 21 $mJ/m^2$, which is smaller than that of Au nanowire with stacking fault energy of 31 $mJ/m^2$. The decrease in the stacking fault energy in the case of the alloy nanowires resulted in stabilization of deformation twinning to a larger critical dimension before transitioning to ordinary plasticity.

TEXT

## 1. Introduction

As the technological limitations on handling nanoscale materials are diminished, attempts to employ such materials into industrial use are being made in a wide range of applications. One of the application field is plasmonic devices such as solar cells, nano-antennas, nano-biosensors, and etc., in which surface plasmon resonances on the nanoscaled metal surfaces by incident light enhance the device performances.[4-12] In order to obtain highly efficient plasmonic devices, it is critical to achieve an ultra-smooth metal surface.[13, 14] Although nanostructured surfaces fabricated by conventional top-

down lithography methods are widely used in plasmonic devices, the inevitable surface imperfections or multi-crystalline defects limit the efficiency of the plasmonic devices fabricated in such a way. On the other hand, single-crystalline metal nanowires fabricated by bottom-up methods are noted to have great potential for the use in advanced plasmonic devices for their surface roughness limited to the atomic scale without significant defects. For this reason, several studies have been conducted for the use of metal nanowires in plasmonic devices.[14, 15] Two of the most popular materials employed in plasmonic devices are Au and Ag, which however show both some limitations: Ag nanowires are prone to ambient contamination by oxidation while Au nanowires suffer from a limited wavelength range for excitation. To overcome such restrictions, topotaxial grown AuAg alloy nanowires are proposed for their superior ambient stability compared to pure Ag as well as a broader range of wavelengths compared to pure Au for inducing the plasmonic effect.[16]

Another aspect in the fabrication of metal nanowires for photonic applications concerns the control over their mechanical properties. Until now, most studies regarding the deformation behavior of nanowires have been conducted on single element nanowires, which is expected to differ from an alloy system.[17-20] For example, the superplastic deformation by partial dislocation mediated plasticity or deformation twinning was observed in defect-free [110] Au nanowires with {111} free surfaces under tensile loading.[17] The sequential creation of leading partial dislocations $\left(b = a/6\langle 11\overline{2}\rangle\right)$ on adjacent crystallographic planes resulted in generation and propagation of twins along the direction of the tensile loading that enabled a larger elongation of beyond 40% compared to typical Au. Such deformation twinning was shown to be highly dependent on the dimensions of the nanowires,[21, 22] so that a critical dimension has been defined at which the deformation mode transits from deformation twining to ordinary dislocation plasticity. The stress required to create leading partial dislocations is smaller than that required for ordinary dislocations due to the smaller Burgers vectors of leading partial dislocation. However, the additional stress needed to form stacking faults for twin formation by leading partial dislocations becomes dominant in a nanowire with dimension larger than the critical dimension, which ultimately limits the deformation twinning. Therefore, one of the main factors in

determining the twin formation in metal nanowires is their stacking fault energy, which is variable depending on the selected material. That relation is also analytically defined as

$$D_C = \frac{2\alpha\mu(b_N - b_P)b_P}{\gamma_{SF}},$$  (1)

where $D_C$ is the critical dimension, α is 0.5 for edge dislocations, $\mu$ is the shear modulus, $\gamma_{SF}$ is the stacking fault energy, and $b_N$ and $b_P$ are the magnitudes of the Burgers vectors for ordinary and leading partial dislocations.[19, 21, 23, 24] Concerning [110] Au nanowires, the stacking fault energy is 31 mJ/m$^2$,[25] resulting in a calculated critical diameter around 30 nm, to be compared with the experimental value around 170 nm.[19]

Once two metals form the alloy, the stacking fault energy is calculated to be in the range between the values of the individual metal components depending on the composition of the alloy. Simply, as a rule of thumb, the AuAg alloy nanowires with composition ratio of 50:50 will have stacking fault energy of 24.5 mJ/m$^2$, where stacking fault energies of Au and Ag are 31 mJ/m$^2$ and 18 mJ/m$^2$, respectively.[25] The decrease in stacking fault energy will result in the increase in critical dimension as expected, according to the equation (1). For more precise prediction, the expected critical dimensions of AuAg alloy nanowires can be calculated and plotted for the different alloy composition ratio using the reported stacking fault energy values obtained by DFT calculation in the reference study by Kaufman *et al.*[25], as shown in Figure 1. Indeed, the stacking fault energy decreases as the weight percentage of Au in AuAg alloys decreases, which increases the calculated critical dimension for deformation twining. For example, an AuAg alloy nanowire with composition ratio of 30:70 has stacking fault energy of 21 mJ/m$^2$, which corresponds to a critical dimension of around 45 nm. This calculated value is around 1.5 times larger than that of pure Au nanowires, which, in other words, implies that deformation twinning will be stabilized to a larger critical dimension before transitioning to ordinary plasticity in the alloyed nanowires in comparison to single element nanowires. In this study, we performed *in-situ* tensile tests of $Au_{30}Ag_{70}$ alloy nanowires and experimentally confirmed that the deformation twinning of alloyed nanowires occurs even in much larger dimension compared to that of single element nanowires.
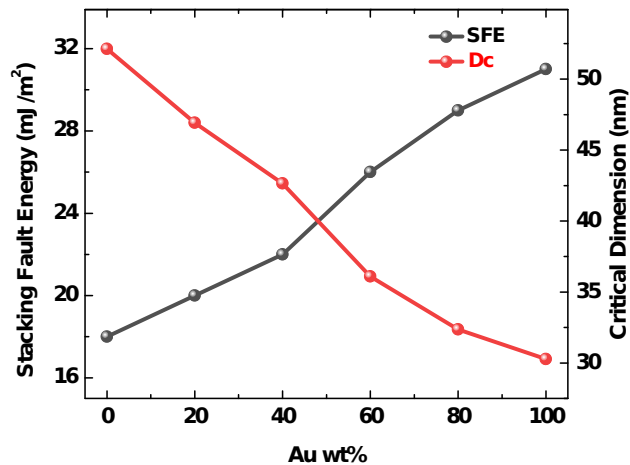
**Figure 1.** Estimated stacking fault energy and the corresponding calculated critical dimensions of AuAg alloy nanowires plotted for various Au weight percentage.

## 2. Experimental

### 2.1. Synthesis of $Au_{30}Ag_{70}$ alloy nanowires

The $Au_{30}Ag_{70}$ alloy nanowires are synthesized by using a topotaxial growth method.[16] Single crystalline Au nanowires are grown epitaxially onto $SrTiO_3$ substrate with (110) orientation by using conventional vapor transport method. Relatively low range of Au atom flux (Ar flow rate about 100 sccm) is utilized for vertical growth of the Au nanowires. After the Au nanowires are synthesized, Ag vapor is supplied while maintaining the substrate temperature at 800 °C. The time of Ag vapor flow is used to control the ratio of Au to Ag. In this study, Ag vapor supply time of 5 min is chosen for the synthesis of $Au_{30}Ag_{70}$ alloy nanowires. The fabricated $Au_{30}Ag_{70}$ nanowires are then analyzed using various techniques to confirm their compositions. The high resolution transmission electron microscopy (HRTEM) and corresponding fast Fourier transform (FFT) pattern images (Tecnai G2 F30 S-Twin (FEI)), as shown in the Figure 2(a) and (b), confirmed that the $Au_{30}Ag_{70}$ nanowires are single crystalline grown in [110] direction. The selected area diffraction (SAD) pattern image (Figure 2(c)) and TEM line energy dispersive X-ray spectroscopy (EDS) (Figure 2(d)) analyses further confirmed the crystallinity of the $Au_{30}Ag_{70}$ alloy nanowires.

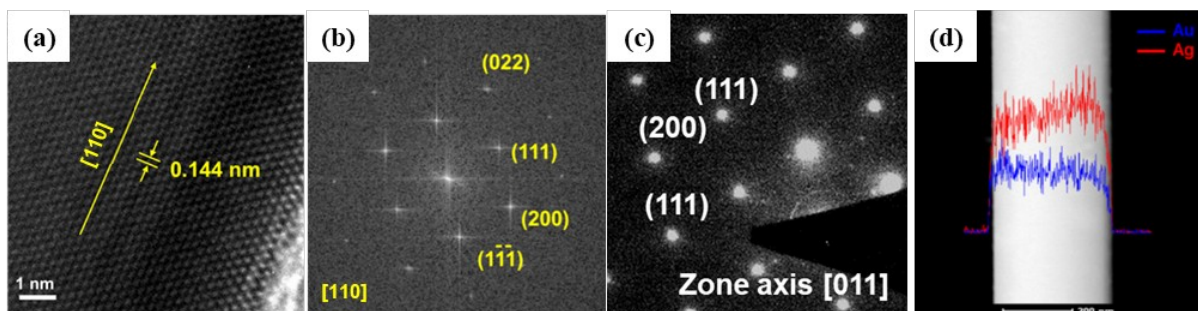**Figure 2.** Analysis of fabricated $Au_{30}Ag_{70}$ alloy nanowires. (a) HRTEM image, (b) FFT pattern image, (c) SAD pattern image and (d) TEM line EDS

## 2.2. In-situ tensile test using PTP

The fabricated $Au_{30}Ag_{70}$ alloy nanowires are loaded onto Push-to-Pull (PTP) device (Hysitron) using optic-probe station. First, a tungsten tip is used to apply a small amount of epoxy onto sample loading section of the PTP. Then, a separate tungsten tip is used to pick up a vertically grown $Au_{30}Ag_{70}$ nanowire and transferred to the PTP. As the epoxy hardens, the $Au_{30}Ag_{70}$ NW is fixed onto the PTP device. Finally, the PTP device is mounted onto 90° angled holder for in-situ tensile testing using pico-indenter (Hysitron, PI-87), as shown in the Figure 3 (a). Flat punch tip with diameter of 13 μm is used to indent the rounded head of the PTP, which initiates the movement of the mobile part of the PTP device to translate the indentation loading into tensile loading at the nanowire mounted area, as shown in the Figure 3 (b). Because each of the PTP devices have their own stiffness values, the pure load applied onto the nanowire can be calculated by subtracting the PTP load, which is the value measured after the nanowire fracture, from the total load. From the load-displacement data measured by indentation using PTP device, stress-strain curve can be plotted using the initial length and cross-sectional surface area of the nanowire. *In-situ* SEM images and the stress-strain results on the tested nanowires are shown in the next section.
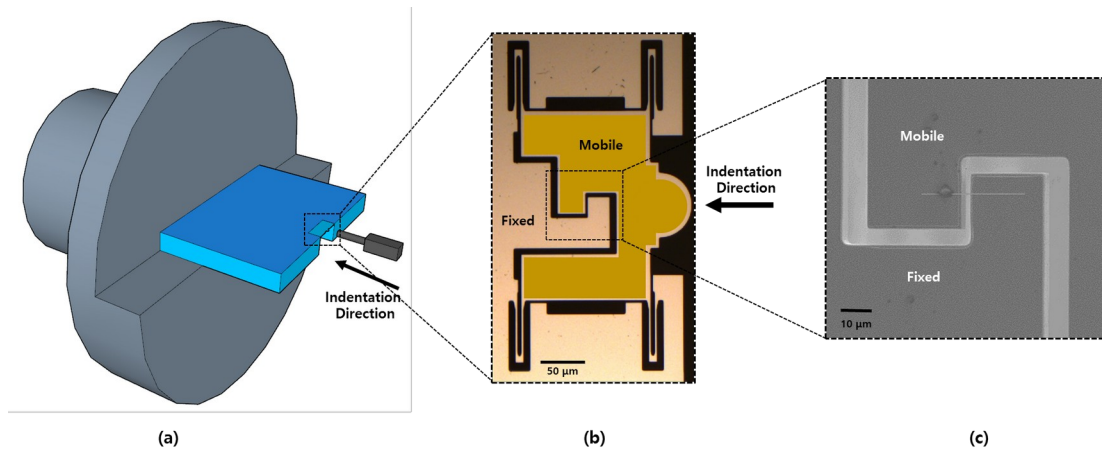
**Figure 3. (a)** PTP mounted onto 90° holder for indentation using pico-indenter, (b) schematic of PTP device, (c) loaded $Au_{30}Ag_{70}$ NW onto the mounted section of the PTP device.
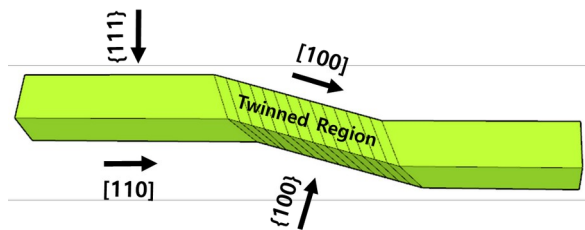
## 3. Results and Discussion



**Figure 4.** Schematic illustrating the orientation change when deformation twinning occurs in a $Au_{30}Ag_{70}$ nanowire.

The $Au_{30}Ag_{70}$ nanowires used in this study are grown in [110] orientation and have {111} side surfaces as shown in Figure 4. When deformation twinning occurs and propagates along the length of a nanowire, the crystallographic orientation changes from [110] to [100] and the free surface orientation changes from {111} to {111}, which tilts the nanowire by around 18° away from the axis of un-twinned nanowires.[19, 26] Therefore, the most direct and clearest method to observe the deformation twinning is to monitor the orientation change of the nanowires during the tensile deformation. In order to confirm the deformation behavior of $Au_{30}Ag_{70}$ alloy nanowires, *in-situ* tensile tests were performed with $Au_{30}Ag_{70}$ alloy nanowires with varying diameters ranging from 319 nm to 486 nm inside a SEM chamber using the PTP setup introduced in the above section. In our previous

report, the critical dimension of Au nanowires was experimentally observed to be ~170 nm, above which ordinary dislocation plasticity occurred accompanying the localized necking followed by sudden failure.[19] Therefore, the tensile tests were performed on nanowires with diameter larger than ~170 nm.

Snapshots during the in-situ SEM tensile deformation of $Au_{30}Ag_{70}$ alloy nanowire with the diameter of 319 nm are shown in Figure 5(a). Interestingly, the $Au_{30}Ag_{70}$ alloy nanowire clearly showed a superplastic behavior via deformation twinning up to 35% before being unloaded even though the dimension of the alloy nanowire was much larger than the critical dimension of Au nanowires, ~170 nm. Instead of localized necking and sudden fracture, which is expected for the Au nanowires with similar dimensions, deformation twinning started at around 4% strain and propagated along the length of $Au_{30}Ag_{70}$ alloy nanowire as indicated by the white arrows in the Figure 5(a). Post-deformation analysis provided further evidence for the deformation twinning of the alloy nanowires. Figure 5 (b) shows the TEM image of the $Au_{30}Ag_{70}$ alloy nanowire with the diameter of 319 nm after the tensile test, where section A and B indicated by white circles corresponds to the un-twinned and twinned regions. TEM analysis confirmed that the diffraction patterns of the twinned and un-twinned regions have the expected twin orientations as indicated in the inset of Figure 5(b). During the deformation twinning, the Au30Ag70 nanowire's rhombic cross-section with {111} free surface re-oriented to the rectangular cross-section with {111} free surfaces and the nanowire's orientation also changed from [110] to [100], which resulted in a reduction of the nanowire diameter and different diffraction patterns between twinned and un-twinned regions.
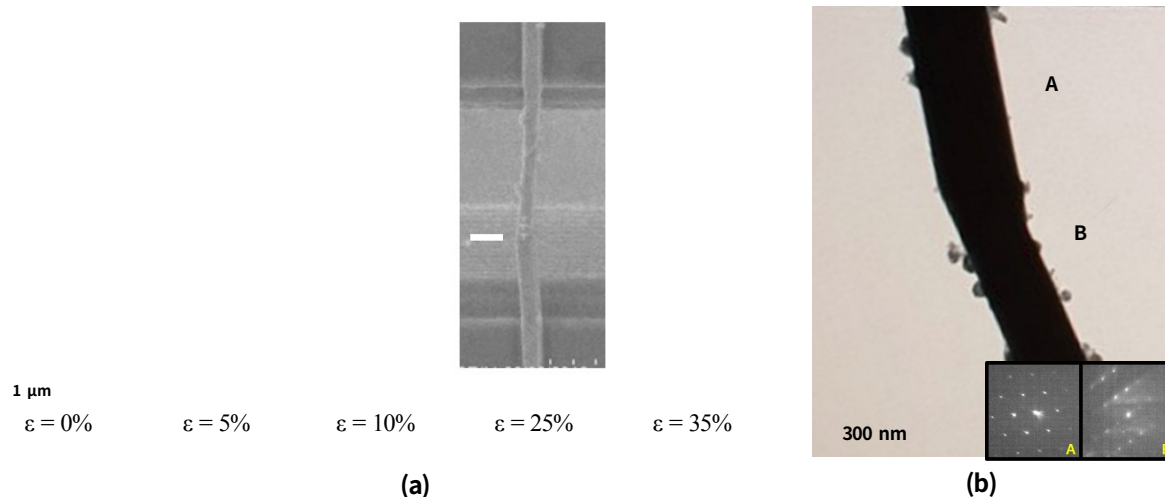
**Figure 5.** (a) *In-situ* tensile testing SEM images of Au$_{30}$Ag$_{70}$ alloy nanowire and (b) post-deformation TEM image of the twinned Au$_{30}$Ag$_{70}$ alloy nanowire.

Stress-strain plot of the Au$_{30}$Ag$_{70}$ alloy nanowire with the diameter of 319 nm is shown in Figure 6. The elastic limit of the alloy nanowire is measured to be 3.93%, which matches the results from previously reported experimental studies on Au nanowires with the same orientation as the alloy nanowires analyzed here.[19] Once the twinning is initiated upon passing the elastic limit, sudden drop of stress occurred, followed by plastic deformation at much lower stress *via* propagation of twins. The yield stress, at which the onset of twin propagation occurred, is measured to be 1.20 GPa, which is relatively closer to the theoretical strengths of Au (1.8 GPa) and Ag (2.4 GPa)[27] compared to bulk strengths of Au (110~230 MPa) and Ag (140~380 MPa).[28] The high experimental strength of the nanowire is attributed to the defect-free state of the Au$_{30}$Ag$_{70}$ alloy nanowires, where significantly higher stress is required for the nucleation of leading partial dislocation for twin formation from the surface. It is known that Au and Ag have similar atomic radius of ~0.14 nm.[29] In addition, the lattice spacing of the Au$_{30}$Ag$_{70}$ alloy nanowires in [110] direction was measured to be 0.144 nm (Figure 2(a)), which is very close with those of Au and Ag. Therefore, significant lattice distortion in the defect-free alloy nanowires will not occur and thus measured yield strength values similar to those of pure Au or Ag are expected. However, once the twin propagation is initiated, the stress needed for plasticity is significantly reduced because the nucleation of initial leading partial dislocation created slip step at

the surface of the nanowire where local stress concentration occurred upon continuous tensile loading of the nanowire, which, in turn, resulted in much easier nucleation of subsequent leading partial dislocations on adjacent planes. The evaluated Young's modulus from the elastic region of the stress-strain curve in Figure 6 is measured to be 35.7 GPa, which is comparable to the expected values of Ag (84 GPa) and Au (78 GPa).[28] The difference in Young's modulus of the tested alloy nanowires from the theoretical values of Au and Ag might be resulted from the misalignment of alloy nanowires on PTPs. Therefore, there might be a small gap between the experimentally determined critical dimension for deformation twining in this study and that of samples tested in an ideal condition.
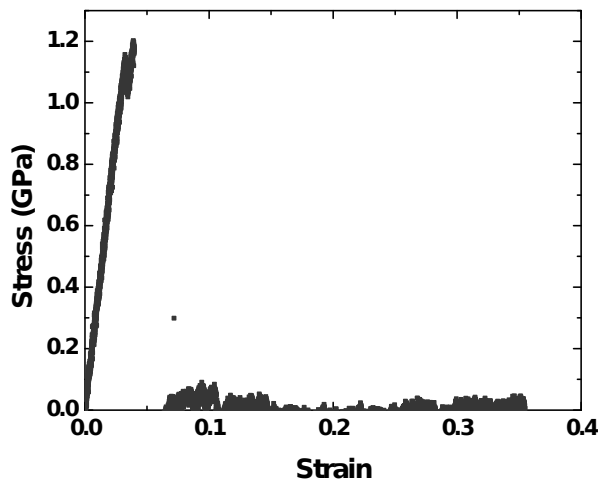


Figure 6. Stress-strain curve of $Au_{30}Ag_{70}$ alloy nanowire tested under tension using PTP system.

Deformation modes of the $Au_{30}Ag_{70}$ alloy nanowires with different diameters are summarized in Table 01. The critical dimension of the $Au_{30}Ag_{70}$ alloy nanowires, where the deformation mode transitions from deformation twinning to ordinary dislocation plasticity, was experimentally observed to be ~333 nm. The critical dimension of $Au_{30}Ag_{70}$ alloy nanowire is around 2 times larger than that observed for the Au nanowires with identical crystalline structure. The increased critical dimension can be attributed to the decrease in stacking fault energy as described in the above sections. According to the equation (1), the stress needed to nucleate the leading partial dislocation accompanying the

formation of stacking fault become larger than that needed to nucleate the ordinary dislocation as the diameter of nanowires increases beyond the critical dimension. Therefore, the critical dimension for deformation twinning can be increased by lowering the stacking fault energy of the material system. In the case of the $Au_{30}Ag_{70}$ alloy, the stacking fault energy is ~1.5 times smaller than that of pure Au, as shown in Figure 1, which consequently resulted in a two-fold larger critical dimension as experimentally observed in this study. Thus, thanks to an increased critical dimension for deformation twinning that enlarges the possibilities in the selection of nanowire dimensions to be utilized, the alloy nanowire system can represent an option for applications involving the use of nanowires in devices requiring high deformability along with high chemical stability. The difference in sidewall orientation of nanowires causes a different surface energy that acts as an energy barrier for twin deformation. Therefore, the critical dimension will vary as the sidewall orientation of alloy nanowires is changed; the study on the deformation behavior of metal nanowires with different sidewall orientation will be the topic of our future work.

| AuAg Alloy NW Diameter | 319 nm | 333 nm | 486 nm | 537 nm |
|---|---|---|---|---|
| Deformation Mode | Deformation twinning | Deformation twinning | Ordinary dislocation plasticity | Ordinary dislocation plasticity |

**Table 01.** Summary of different deformation modes of $Au_{30}Ag_{70}$ alloy nanowires with various diameters.

## 4. Conclusions

In this work, we have demonstrated for the first time that the alloyed nanowires show different deformation twinning behavior compared to single element nanowires because of the difference in stacking fault energies. Topotaxially grown $Au_{30}Ag_{70}$ nanowires with varying diameters were tested in tension using *in-situ* using PTP devices. We observed that $Au_{30}Ag_{70}$ nanowires with a ~319 nm diameter undergo a deformation *via* twinning, showing superplastic deformation up to 35 % strain

before being unloaded. The expected change in orientation of the nanowire from [110] to [100] during deformation twinning was further confirmed by TEM analysis. Defect-free $Au_{30}Ag_{70}$ alloy nanowires also showed high strength of 1.20 GPa, which is closer to the theoretical strengths of Au and Ag compared to their bulk strengths. By performing *in-situ* tensile tests, the critical dimension for transition from deformation twinning to ordinary plasticity was confirmed to be 333 nm, which was ~2 times larger than that of previously reported single element Au nanowires with same geometry. The increased critical dimension was attributed to the decrease in stacking fault energy in the alloy system that stabilized deformation twinning up to larger critical dimensions. Therefore, such alloy nanowires showing the superplastic deformation at much larger dimension than single element nanowires can be proposed for diverse applications requiring high strength and deformability as well high chemical stability.

ACKNOWLEDGEMENTS

REFERENCES

1.  B. Hwang, S. Lim, M. Park, and S. M. Han, *RSC Advances*, 2017, **7**, 8186-8191

2.  C. An, S. Kim, H. Lee, and B. Hwang, *Journal of Materials Chemistry C,* 2017, **5**, 4804-4809

3.  B. Hwang, W. Kim, J. Kim, S. Lee, S. Lim, S. Kim, S.H. Oh, S. Ryu, and S. M. Han, *Nano letters,* 2017, **17**, 4740-4745

4.  J. Seidel, S. Grafström and L. Eng, *Physical Review Letters*, 2005, **94**, 177401.

5.  W. Cai, J. S. White and M. L. Brongersma, *Nano Letters*, 2009, **9**, 4403-4411.

6.  D.-S. Kim, J. Heo, S.-H. Ahn, S. W. Han, W. S. Yun and Z. H. Kim, *Nano Letters*, 2009, **9**, 3619-3625.

7.  A. Kinkhabwala, Z. Yu, S. Fan, Y. Avlasevich, K. Müllen and W. E. Moerner, *Nature Photonics*, 2009, **3**, 654.

8.  P. A. Mistark, S. Park, S. E. Yalcin, D. H. Lee, O. Yavuzcetin, M. T. Tuominen, T. P. Russell and M. Achermann, *ACS Nano*, 2009, **3**, 3987-3992.

9.  R. A. Pala, J. White, E. Barnard, J. Liu and M. L. Brongersma, *Advanced Materials*, 2009, **21**, 3504-3509.

10. H. A. Atwater and A. Polman, *Nature Materials*, 2010, **9**, 205.

11. P. Christopher, H. Xin and S. Linic, *Nature Chemistry*, 2011, **3**, 467.

12. Y. C. Jun, K. C. Y. Huang and M. L. Brongersma, *Nature Communications*, 2011, **2**, 283.

13. J.-S. Huang, V. Callegari, P. Geisler, C. Brüning, J. Kern, J. C. Prangsma, X. Wu, T. Feichtner, J. Ziegler, P. Weinmann, M. Kamp, A. Forchel, P. Biagioni, U. Sennhauser and B. Hecht, *Nature Communications*, 2010, **1**, 150.

14. P. Nagpal, N. C. Lindquist, S.-H. Oh and D. J. Norris, *Science*, 2009, **325**, 594-597.

15. I. Yoon, T. Kang, W. Choi, J. Kim, Y. Yoo, S.-W. Joo, Q. H. Park, H. Ihee and B. Kim, *Journal of the American Chemical Society*, 2009, **131**, 758-762.

16. H. Lee, Y. Yoo, T. Kang, J. In, M.-K. Seo and B. Kim, *Small*, 2012, **8**, 1527-1533.

17. J.-H. Seo, Y. Yoo, N.-Y. Park, S.-W. Yoon, H. Lee, S. Han, S.-W. Lee, T.-Y. Seong, S.-C. Lee, K.-B. Lee, P.-R. Cha, H. S. Park, B. Kim and J.-P. Ahn, *Nano Letters*, 2011, **11**, 3499-3502.

18. J.-H. Seo, H. S. Park, Y. Yoo, T.-Y. Seong, J. Li, J.-P. Ahn, B. Kim and I.-S. Choi, *Nano Letters*, 2013, **13**, 5112-5116.

19. B. Hwang, M. Kang, S. Lee, C. R. Weinberger, P. Loya, J. Lou, S. H. Oh, B. Kim and S. M. Han, *Nanoscale*, 2015, **7**, 15657-15664.

20. A. Sedlmayr, E. Bitzek, D. S. Gianola, G. Richter, R. Mönig and O. Kraft, *Acta Materialia*, 2012, **60**, 3985-3993.

21. M. Chen, E. Ma, K. J. Hemker, H. Sheng, Y. Wang and X. Cheng, *Science*, 2003, **300**, 1275-1277.

22. J.-Y. Zhang, G. Liu, R. H. Wang, J. Li, J. Sun and E. Ma, *Physical Review B*, 2010, **81**, 172104.

23. K. P. D. Lagerlöf, J. Castaing, P. Pirouz and A. H. Heuer, *Philosophical Magazine A*, 2002, **82**, 2841-2854.

24. J. P. Hirth and J. Lothe, *Theory of dislocations*, Krieger Pub. Co., Malabar, FL, 1992.

25. J. L. Kaufman, G. S. Pomrehn, A. Pribram-Jones, R. Mahjoub, M. Ferry, K. J. Laws and L. Bassman, *Physical Review B*, 2017, **95**, 094112.

26. E. Bitzek, *Journal of Solid Mechanics and Materials Engineering*, 2012, **6**, 99-105.

27. S. Ogata, J. Li, N. Hirosaki, Y. Shibutani and S. Yip, *Physical Review B*, 2004, **70**, 104104.

28. A. M. Howatson, Lund, P. G., Todd, J. D., *Engineering tables and data*, Chapman and Hall, London, 1972.

29. B. Cordero, V. Gómez, A. E. Platero-Prats, M. Revés, J. Echeverría, E. Cremades, F. Barragán and S. Alvarez, *Dalton Transactions*, 2008, DOI: 10.1039/B801115J, 2832-2838.